Available online at www.elixirpublishers.com (Elixir International Journal)

Thermal Engineering

Elixir Thermal Engg. 122 (2018) 51615-51620

ISSN: 2229-712X

Novel Natural Convection Process: Indirect Solar Dryer Built with Spherical Concentrators. Application to Tomato Drying.

Thierry S. Maurice Ky, Boureima Dianda, Emmanuel Ouedraogo, Salifou Ouedraogo and Dieudonné J. Bathiebo
Laboratory L.E.T.RE, University Ouaga I Pr Joseph KI-ZERBO, Ouagadougou – Burkina Faso

ARTICLE INFO

Article history:
Received: 11July 2018;
Received in revised form:
20 August 2018;
Accepted: 29 August 2018;

Keywords
Natural Convection,
Tomato,
Solar Dryer,
Spherical Concentrator,
Steady Collector,
Hot-Spot Theory.

ABSTRACT
This study presents a novel natural convection process. A prototype of an indirect solar dryer, with its collector made of hemispherical concentrators had been realized and studied with the idea of obtaining higher temperature in the drying chamber, and this with a steady non tracking collector. The patented collector is based on the hot-spot theory. Measurements had been conducted for all critical period of the year. The result seemed conclusive with temperature improvement in steady non tracking collectors, and suggests further investigation of the hot-spot theory, by conceiving a mathematical model and by deepening the experiment outcomes for a best thermodynamic study.

1. Introduction

For some time, solar dryers had been composed of fixed collectors to avoid solar tracking. Solar tracking seems to be the greatest problem in our countries with very powerful winds that can bring huge damages to solar installations that use trackers. Also, with the mathematic and the robotic aspects behind trackers dimensioning, finding specialists to take care of installations using these trackers had been found challenging [1]. Somehow, tracking system is usually involved when there is concentration for a higher temperature. Most of those concentrators function with the conditions sine qua none of having the sunrays coming perpendicularly to their exposition surface.

There are many reviews comparing different solar fixed collectors: open, direct or indirect sun dryers, active, passive or mixed drying mode, with or without greenhouse effect, etc. [2-7]. Those fixed collectors are built with absorbers composed of black plates with fins or not. These collectors functioning principle is simple: the absorber, as a black body, gets the heat from the sun by radiation. The air is therefore introduced to collect that heat by convection. If the air is forced by a pumping device or a fan, we are in an active mode. If not, the air therefore moves due to the change of its density getting into a thermo-siphon effect, which is called natural convection. Most of the dryers has a glass coverage to retain infrared rays coming from the sun and increasing de facto the heat [8].

The novelty in the proposed system here is the total lack of absorber. As patented by Ky and Bathiebo [9], the system relies on fixed concentrators that don't need sun-tracking. The hemispherical concentrator or Solar Bowl had been ostensibly presented and studied [10-12]. Its geometric or geometric mean concentration ratio had been redefined [13; 14]. Then, earlier publication showed the generation of a hot-spot to consider for the new system [15]. Interesting temperatures had been obtained.

Concretely, the new system has a fixed non-tracking collector built with hemispherical concentrators, without any absorber, and with the purpose of getting a higher range of temperatures.

2. Description of the solar dryer

The prototype is composed of a collector, a chamber and a chimney.

The collector is built with three channels of hemispherical concentrators. Each channel is composed of 10 concentrators aligned North-South and making 12° angle with the horizontal with respect to the latitude angle of the locality, Ouagadougou (Fig. 1 and 2).

Figure 1. Picture of the system: collector.

Figure 2. Picture of the system: chamber.

Tele: +226 70 88 08 58
E-mail address: thierrysmky@gmail.com

Air flows from the admission inlet through the three channels, and it gains heat by passing through them to the chamber. The chamber is glass wool insulated. The air circulates by natural convection, gaining in speed with the temperature. Then, it dries the tomato slices seating on the trays before leaving the chamber through the chimney as indicated on the Fig. 3. The trays are built with aluminum grids to allow airflow through the disposed products.

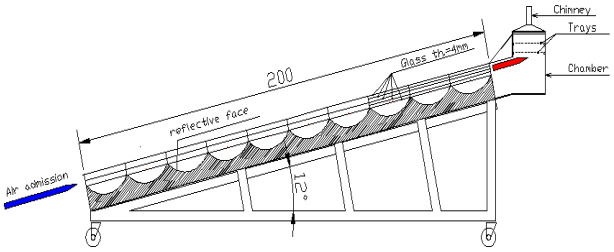

Figure 3. Descriptive scheme of the system.

Each of the 3 channels is composed of ten vertically truncated hemispherical concentrators. The truncating is made to allow air transition through the concentrators. 4 mm thick glasses are disposed to create bands through which air circulates. The first 7 concentrators have 2 bands while the last 3 ones have 4 bands. Although the total glazing surface of the collector is 2 m^2, the effective surface can be considered as equal to the sum of each channel concentrators' width * 2 m length of the channels. That gives the collector effective surface equal 1.46 m^2.

The collector is built using an assembly of 30 plaster bricks spherically-shaped inside as shown on Fig. 4.

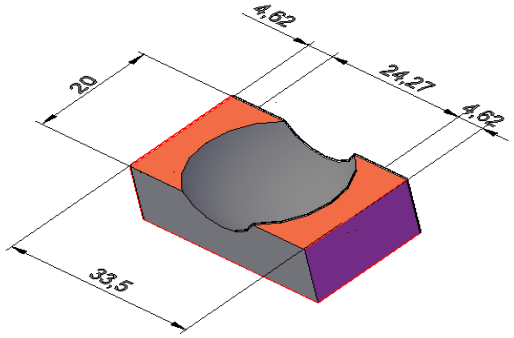

Figure 4. Plaster brick used as hemispherical concentrator.

Each brick is internally mapped with auto-taping reflective material giving a mirror effect. There isn't any absorber or black-painted plate, the only wanted effect is the creation of a hot-spot by the hemispherical concentrator, the inner reflective surface.

The less volume of air is heated, the more it gains in temperature. Therefore, bands are created to allow the air gain heat from the hot-spot corresponding to the real image of the sun after concentration, as described on Fig. 5 and 6.

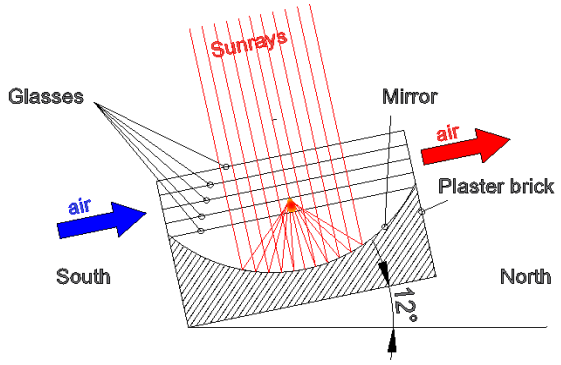

Figure 5. North-South positioning of the concentrator.

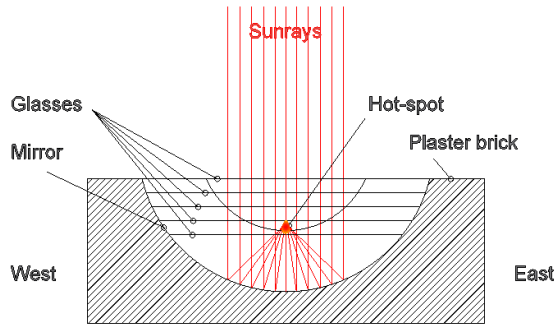

Figure 6. East-West positioning of the concentrator.

As indicated on the next Fig. 7, concentration hot-spot is moving through the first two bands from bottom, showing the extreme position of the hot-spot due to the declination angle during the year.

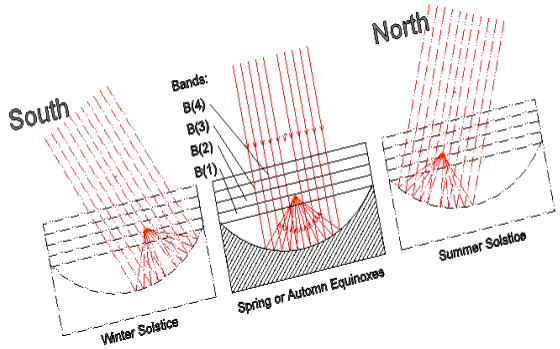

Figure 7. Positioning of the hot-spot with the declination angle.

Figure 8 shows the position of the hot-spot from morning to evening. The extreme position gained in the day depends also of the hour angle and the day of the year, meanwhile the extreme vertical position of the hot-spot on Fig. 8.a and 8.b differs according to the fact of being at the equinoxes (lower) or the solstices (higher).

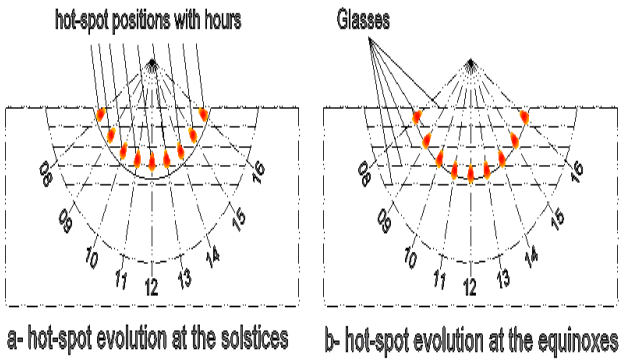

Figure 8. Positioning of the hot-spot during daytime.

3. Functioning principle of the system

The theory had been explained to some point on a previous article, giving the optimal angle defining the hot-spot, the size of the hot-spot in accordance with the concentrator radius and the temperature of the hot-spot in relation to the insolation factor [15]. The hot-spot is considered quasi-steady due to it low velocity (15° angle per hour). The concentration factor of the hot-spot reaching 720, that makes it hot enough to transmit its heat to the air in the considered band by natural convection. The high mixing factor caused by the density-change of air with temperature could be the main reason of the better efficiency of the system compared to usual systems. The air density ρ in kg/m^3 approximatively responds to the following law in constant atmospheric pressure and 0% moisture conditions using the

the perfect gas law:

$$\rho \approx 1.292 \frac{T_0}{T} \quad (01)$$

With T_0=273.15 K.

Hemispherical concentrators are usually used as fixed with mobile receivers. Its exposition area A_{ex} can be calculated using the following equation 2:

$$A_{ex} = \pi R_{op}^2 \lambda \quad (02)$$

With R_{op} the radius of the concentrator opening area and λ the area multiplication factor. This multiplication factor depends on the time angle ω_{sol} equal to zero at noon (1 hour equal 15° angle) and the declination angle δ can be evaluated using the following equation 3 [16]:

$$\delta \approx 23.45 \sin\left(360 \frac{284+n}{365}\right) \quad (03)$$

With n corresponding to the day of the year starting at January 1st.

The multiplication factor can be defined by the following equation 4:

$$\lambda = \cos\delta \cos\omega_{sol} \quad (04)$$

The drawing of a 3D curve in relation to the multiplication factor gives the following Fig. 9.

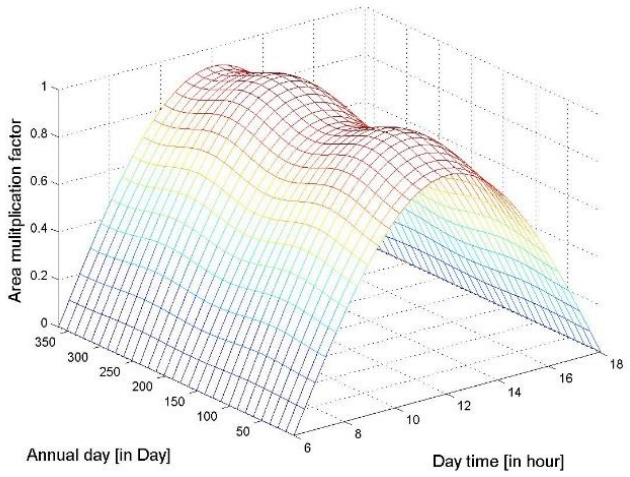

Figure 9. Evolution of area multiplication factor according to the day of the year and the hour of the day.

We can notice that the multiplication factor equal to 1 at noon and at the equinoxes, which corresponds to the days n=81 and n=263 of the year, when the sunrays are parallel to the normal of the exposition area. Moreover, from 8:30 am to 3:30 pm all the year, the multiplication factor is above 0.6, which indicates that we still have sufficient insolation to work with the steady concentrator.

The whole system like usual convective dryers are built and positioned identically with no turning parts, aligned with the geographic North and leaned according to latitude angle or optimum angle for best convection, but due to the fact that the presented system is built with concentrators, final temperature is higher than usual convective dryers.

4. Materials and Methods

To study the system, we used the equipment listed below and adopted the measurement methods referring to it:

- A data logger Midi LOGGER GL200A of GRAPHTEC brand.
- A probe (Outdoor) measures outdoor (or ambient) temperature.
- Probes (B1 to B4) measure the temperatures of each band, from the lowest to the highest one.
- A probe (Chamber) measures enclosed temperature in the chamber.
- Probes (UTr and DTr) measure the temperatures of the trays from Up (UTr) to down (DTr).
- A probe (Chimney) measures the temperature at the chimney.
- A pyranometer SR03-05 of Hukseflux brand measures global insolation.

5. Results and discussions

To best evaluate the dryer performances, it was tested under various climatic and atmospheric conditions, as the dryer works using only direct sunlight.

5.1. Results of November 11, 2017.

In Burkina Faso, November corresponds to the month announcing the ending of the raining season. There are still some clouds in the sky, but the sky is clean and direct sunlight easily gets to the ground. Somehow, we long pass the autumn equinox and are heading to the winter solstice, which gives a declination angle quite high enough (18.17° south with the normal of the collector) to have a lower sun passing south to the zenith. This gives us the following global insolation curve for November 11th (Fig. 10).

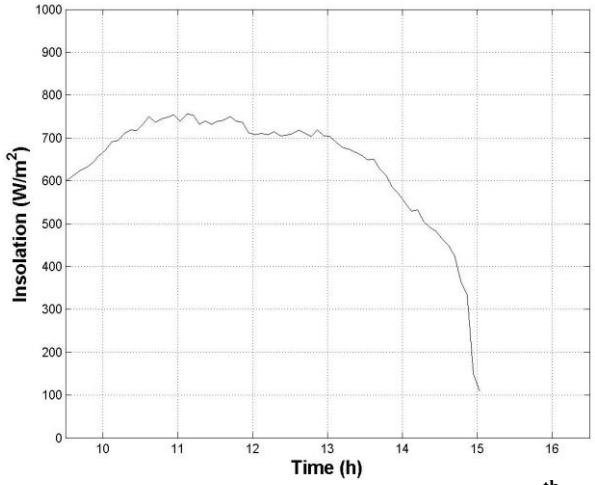

Figure 10. Global insolation curve of November 11th, 2017.

The global insolation curve of November 11th starts with 600 W/m2 at 9:30 am when the data collection started, passes through a pic of 755 W/m2 at 11:00 am. Then with some clouds coverage, we saw a drop of the insolation to 311W/m2 at 3:00 pm when the system was gained by shadow.

The temperatures measurement leads to the drawing of the following curves (Fig. 11).

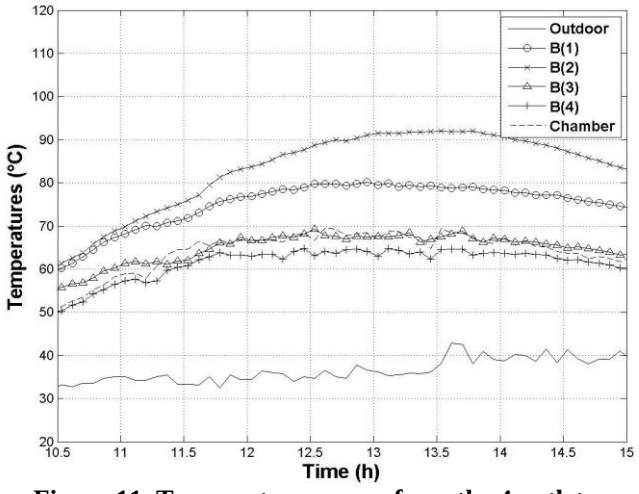

Figure 11. Temperature curves from the 4 outlets, outdoor and the dryer chamber for November 11, 2017 measurement.

The Probes were placed to measure the four outlets of the middle channel, the outdoor and the chamber's temperatures of the dryer as indicated in Fig.11 above. All temperatures rise at 10:30 am, go through a maximum and fall at 03:00 pm. The highest temperature (92°C) is found in the second outlet, due to the declination which enables the sun spot to travel through the first one.

The air temperature in the chamber evolves between 50 and 70°C.

5.2. Results of March 27, 2018.

This month corresponds to the hottest of the year. We usually are out of the period when suspended particles from Niger or Mali cover the sky with dust. The declination angle is equal to 2°, making the zenithal sun rays almost aligned with the normal of the exposition plan of the dryer. That gives the insolation curve as indicated on Fig. 12.

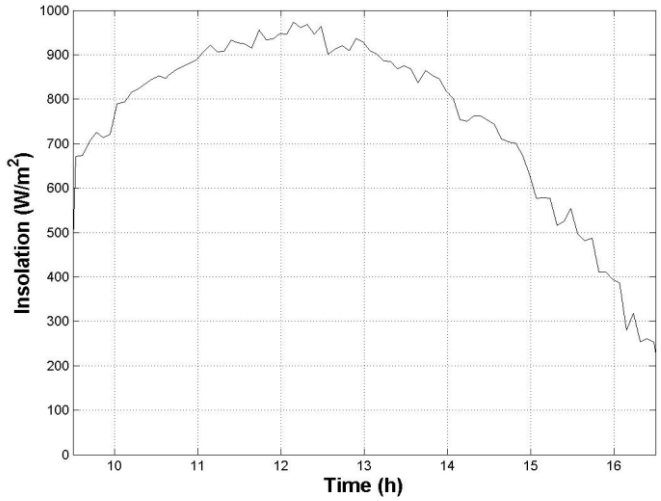

Figure 12. Global insolation curve of March 27, 2018.

The global insolation curve of March 27 starts with 675 W/m^2 at 9:30 am, pass through a pic of 972 W/m^2 at 1:30 pm, then goes down to 240W/m^2 at 4:30 pm when measurement is stopped.

The temperatures measurement of that day leads to the drawing of the following curves (Fig. 13).

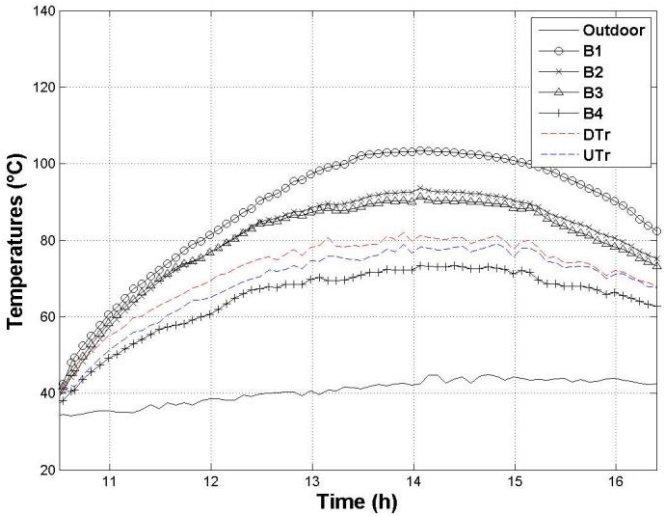

Figure 13. Temperature curves from the 4 outlets, outdoor and the upper and Down trays of the dryer for March 27, 2018 measurement.

Like the first measurement, probes were placed to measure the four outlets of the middle channel and the outdoor temperatures. This time, we also measured the trays' temperatures of the dryer as indicated in the previous figure. All temperatures rise at 10:30 am, go through a maximum and fall at 04:30 pm. The highest temperature (103.4°C) is found in the first outlet a 14:00 pm due to the declination which enables the sun spot to travel through it as previously explained by Fig. 13.

The air temperatures at the trays evolves between 40 and 82°C at the same period of 10:30 am to 04:30 pm, with the lower tray temperature (DTr) slightly higher than that of the upper one (UTr).

5.3. Results of June 08 and 09, 2018.

June is the month announcing the beginning of the raining season. There are always some clouds in the sky so that direct sunlight cannot easily get to the ground. The spring equinox is gone long ago, and we are heading to the summer solstice. The declination angle is still high enough (22° North with the normal) to have a sun passing high in the sky, and actually the sun had shifted North to the zenith. This gives us the following global insolation for June 08 and 09, 2018 (Fig. 14). June 08 had a better insolation than 09 which was cloudy all day.

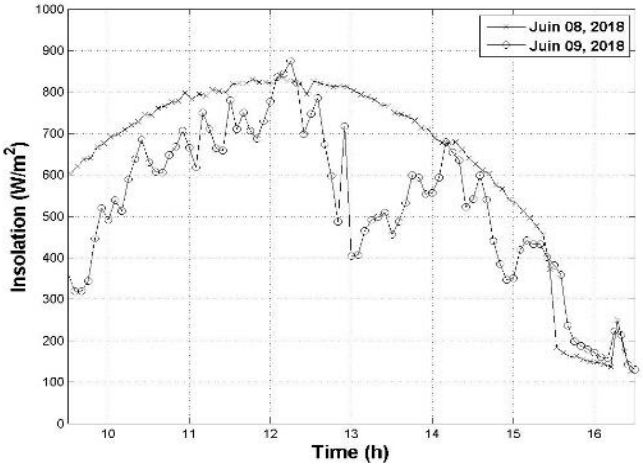

Figure 14. Global insolation curves of June 08 and 09, 2018.

This global insolation curve of June 08 starts with 600 W/m2 at 9:30 am when the data collection started, pass through a pic of 839 W/m^2 at 12:07 pm. Then drop to 455W/m^2 at 3:22 pm when the system was gained by shadow.

That of June 09 follows the same pattern, but is interrupted with a cloudy sky. It starts with 350 W/m^2 at 9:30 am, get a pic of 874W/m^2 at 12:15 pm and drop to 359W/m^2 at 3:35 pm when the dryer is reached by shadow.

The temperatures measurement of June 08 lead to the drawing of the following curves (Fig. 15).

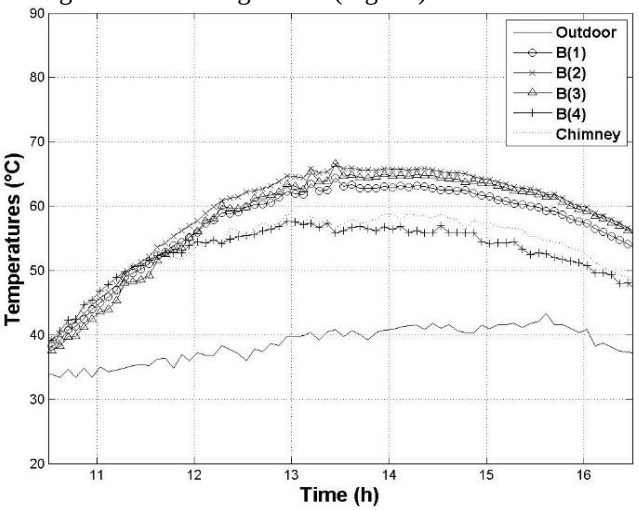

Figure 15. Temperature curves from the 4 outlets, outdoor and the dryer chimney for June 08, 2018 measurement.

As the other previous measurements, probes were placed to measure the four outlets of the middle channel, the outdoor and chimney temperatures of the dryer as indicated in the previous figure. All temperatures rise at 10:30 am, go through a maximum and fall at 04:30 pm. The highest temperature (66.6°C) is found in the second outlet a 13:27 pm due to the declination. Somehow, the gap between temperatures of 1st to 3rd outlet is consequently reduced. Only the 4th outlet has lower temperature, but still between 40°C and 60°C, just like the air temperature at the chimney as indicated by Fig. 15.

The temperatures measurement of June 09 lead to the drawing of the following curves (Fig. 16).

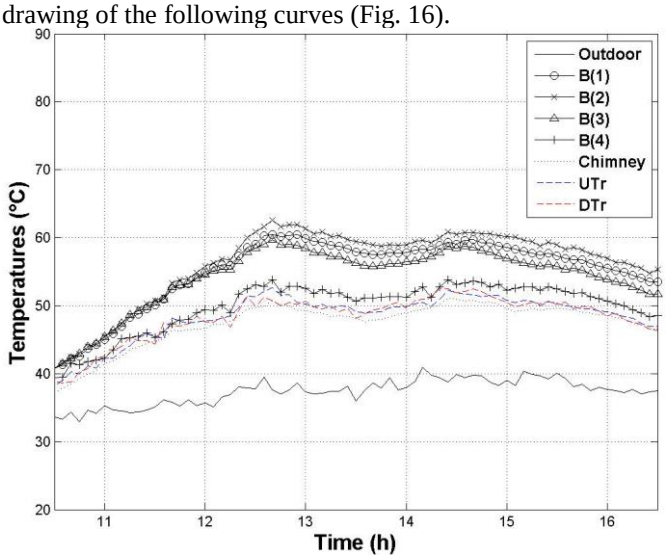

Figure 16. Temperature curves from the 4 outlets, outdoor, Chimney and the two trays of the dryer for June 09, 2018 measurement.

As usual, probes were placed to measure the air temperature from the four outlets of the middle channel, the outdoor, the two trays and chimney of the dryer as indicated in the previous figure. All temperatures rise at 10:30 am, go through a maximum and fall at 04:30 pm. The highest temperature (62.6°C) is found in the second outlet a 12:40 pm due to the declination. The gap between temperatures of 1st to 3rd outlet is also reduced if compared to the temperatures of June 08. Only the 4th outlet has lower temperature, but still between 40°C and 55°C, just like the air temperature at the two trays and the chimney as indicated by Fig. 16. The gap between the two trays and the 4th outlet is less than or equal to 4°C.

The two trays were charged with tomato slices 5mm thick as shown on the following Fig. 17 and 18, and probes to measure temperatures from trays were placed around 3 cm above each tray.

Figure 17. Tomato slides before drying.

229.7g of tomatoes slices 5 mm thick were charged from 09:30 am to 4:30 pm on June 08 and from 09:30 am to 01:00pm on June 09. We observed a total weight drop of 56% the first day, and the final remaining weight was of 17% of the initial mass at 1:00 pm of June 09.

Figure 18. Tomato slides after drying.

5.4. Discussions

From the measurement results, we can see that temperature curve shapes are clock-like just as the insolation curves. Some of the bands have higher temperature, which is consistent with the idea of the band having the hot-spot being much hotter than the others.

The data concerning tomato drying are: Initial water content equal 96%, finale moisture content after drying process should be equal to 10% and maximum allowance temperature equal 60°C [3]. Hence the given temperatures in the chamber, around the trays or at the chimney can be summarized as follow (Table 1).

Table 1. Data recap comparing each period's insolation and temperature values.

Date	Measurement location	Insolation max value (W/m^2)	Temperature frame (°C)
Nov. 11th, 2017	Chamber	755	50 - 70
Mar. 27th, 2018	Trays	972	40 - 82
June 08th, 2018	Chimney	839	40 – 60
June 09th, 2018	Trays & Chimney	874	40 - 55

From those data, we notice that November 11th and March 27th temperatures are higher than those required to dry tomatoes. Using the system to dry tomatoes at that period would require precautions such as mixing chamber-admitted hot air with ambient air to lower down that temperature. The system could also be used to dry products using the same range of temperatures or lower like Maize (60°C), Wheat (45°C), Corn (50°C), Rice (50°C), Pulse (40-60°C) or Oil seed (40-60°C) using the same precautionary measures.

However, unlike ordinary dryers, the system could be used to dry products with higher range of temperatures like Green Pea (65°C), Cauliflower (65°C), Carrot (75°C), Green bean (75°C), Sweet Potato (75°C), Potato (75°C), Chilly (65°C), Apricot (65°C), Apple (70°C), Grape (70°C), Banana (70°C), Guava (65°C), Okra (65°C) and Pineapple (65°C). These temperature ranges can even be guaranteed by a selective admittance of the air coming from the hotter band(s) if needed.

6. Conclusion and Perspectives

As presupposed by Ky and Bathiebo [9] in their patent, and the later publication [15], a steady collector made with assembled hemispherical concentrators can improve considerably air heat for solar dryers. Although the proposed system was poorly fabricated, we obtained results from

different time of the year, closer to the equinoxes, to the solstices and also at the beginning and the end of the raining season, meanwhile, in a cloudy day when direct sunrays are reduced. These results are quite interesting to further investigate the system: The temperature ranges allowed to dry 229.7g of tomato slices 5mm thick with total loss of 83% of original weight in 12:30 hours drying time. Furthermore, the temperature ranges obtained at some days and times of the year or in the outlet of some bands of the collector suggest that other products with higher drying recommended temperature could be also dried by the system. After all, the obtained result is confirming the hot-spot theory.

The perspectives are to find a mathematical model of the system for further studies. Also, as suggested in the patent, a chimney solar tower can be built for confirmation and to ease the thermodynamic study.

7. Acknowledgements

The authors gratefully acknowledge the Ministry of Industry, Trade and Handicrafts of Burkina Faso (MICA-Burkina) for having supported the related patent OAPI N°16893 filled by Ky and Bathiebo, and the Family Federation for World Peace and Unification International Headquarter (FFWPU-HQ, South Korea) for resources disposal to accomplish this work.

References

[1]Thierry S. Maurice Ky, Boureima Dianda, Mahamadi Savadogo and Dieudonne Joseph Bathiebo. Basic Mathematics to Robotic for Tracking Systems Used by Autonomous Solar Collectors. International Journal Of Innovative Research In Technology. 2018 4(11):2054-9

[2]N. L. Panwar, S. C. Kaushik and S. Kothari 'State Of The Art On Solar Drying Technology: A Review', Int. J. Renewable Energy Technology, 2012 3(2):107–141.

[3]Om Prakash & Anil Kumar. Historical Review and Recent Trends in Solar Drying Systems, International Journal of Green Energy, 2013 10(7), 690-738

[4]Sahdev, R. K., M. Kumar, and A. K. Dhingra. A Review On Applications Of Greenhouse Drying And Its Performance. Agricultural Engineering International: CIGR Journal, 2016 18 (2):395-412.

[5]Karunesh Kant, Atul Sharma, Amritanshu Shukla (2017). Chapitre 2. Numerical Techniques for Evaluating the Performance of Solar Drying Systems. Green Energy and Technology; 381-402

[6]B.K. Bala, and Debnath Nipa. Solar Drying Technology: Potentials and Developments. Journal of Fundamentals of Renewable Energy and Applications; 2012 2:1-6.

[7]Sumit Tiwari, G. N. Tiwari, I. M. Al-Hela. Development And Recent Trends In Greenhouse Dryer: Renewable and Sustainable Energy Reviews; 2016 65:1048-54.

[8]G. Arunsandeep, Abhay Lingayat, V.P. Chandramohan, V.R.K. Raju & K. Srinivas Reddy. A Numerical Model For Drying Of Spherical Object In An Indirect Type Solar Dryer And Estimating The Drying Time At Different Moisture Level And Air Temperature, International Journal of Green Energy; 2018 pp.1-12

[9]Ky, T. S. M. And Bathiebo, D. J., Capteur Solaire Fixe A Production En Température Elevée. OAPI patent N°16893, BOPI N°02BR2015 P23-24.

[10]El-Refaie, M. F. Ferformance Analysis Of The Stationary-Reflector/Tracking-Absorver Solar Collector. Applied Energy; 1987 28:163-89

[11]Gandhe VB, Venkatesh A, Sriramulu V. Analysis Of A Fixed Spherical Reflector Exposed To Oblique Incident Rays. Energy Conversion Management. 1986; 26:363‑8.

[12]Gandhe VB, Venkatesh A, Sriramulu V. Optical Analysis Of A Cylindrical Absorber In A Fixed Spherical Reflector. Energy. 1986; 11:969‑76.

[13]KY T. S. M., Kam S., Dianda B. and Bathiebo D. J., Optical Analysis Of A Hemispheric Concentrator With A Manual Tracking System For The Declination. Global Journal of Pure and Applied Sciences, 21: 146-154, 2015

[14]KY T. S. M., Dianda B., Ousmane M., Pakouzou B. M., Kam S. and Bathiebo D. J., Optical And Thermal Performance Analysis Of A Steady Spherical Collector With A Crescent-Shaped Rotating Absorber. International Journal of Advanced Engineering Research and Science. Vol. 4 Issue. 4: 234-245, 2017

[15]Thierry S. Maurice Ky, Magloire Pakouzou, Boureima Dianda, Moctar Ousmane, Sié Kam, Dieudonné J. Bathiebo. Air Heating In A Steady Hemispherical Concentrating System For Various Applications. International Journal of Current Research. févr 2018;10(2):65449-54.

[16]P.I. Cooper, The Absorption Of Radiation In Solar Stills. Solar Energy Volume 12 Issue 1969 Pages 333 – 346.